http://dx.doi.org/10.5012/bkcs.2013.34.9.2650

Synthesis of Thermally Stable Mesoporous Alumina by using Bayberry Tannin as Template in Aqueous System

Jing Liu,[†,‡] Fuming Huang,[†,‡] Xuepin Liao,[†,‡,*] and Bi Shi[‡,§]

[†]*Department of Biomass Chemistry and Engineering, Sichuan University, Chengdu 610065, P.R. China*
[*]*E-mail: xpliao@scu.edu.cn*
[‡]*Key Laboratory of Leather Chemistry and Engineering of Ministry of Education, Sichuan University, Chengdu 610065, P.R. China*
[§]*National Engineering Laboratory for Clean Technology of Leather Manufacture, Sichuan University, Chengdu 610065, P.R. China*
Received March 25, 2013, Accepted June 11, 2013

Mesoporous alumina was synthesized using bayberry tannin (BT) as template. This novel synthesis strategy was based on a precipitation method associated with aluminum nitrate as the source of aluminum in an aqueous system. N_2 adsorption/desorption, XRD, SEM and TEM were used to characterize the as-prepared mesoporous alumina. The results showed that the mesoporous alumina possessed crystalline pore wall, high specific surface area, narrow pore distribution and excellent thermal stability. Moreover, the surface area and pore size of the mesoporous alumina can be tuned by changing the experimental parameters. Further, the mesoporous alumina was investigated as the support of palladium catalyst (Pd-Al_2O_3*) for the hydrogenation of propenyl, styrene and linoleic acid. For comparison, the reference catalyst (Pd-Al_2O_3) prepared without barberry tannin was also employed for the catalytic hydrogenation. The experimental results showed that Pd-Al_2O_3* exhibited the superior catalytic performance than Pd-Al_2O_3 for all the investigated substrates, especially for the hydrogenation of linoleic acid with larger molecular.

Key Words : Mesoporous alumina, Bayberry tannin, Template, Thermal stability, Catalyst support

Introduction

Porous aluminas, owing to their thermal, chemical and mechanical stability and low cost, are extensively used in catalysis, adsorption, and separation.[1-3] In general, the control of pore geometry and size is crucial to adjust their performance in these applications, especially in the case of which rely on size or shape selectivity.[4-6] However, the traditional aluminas are commonly prepared through precipitation method and thermal treatment of aluminum oxide-hydroxide precursors.[7] These traditional porous aluminas usually have the disadvantages of low surface area and uncontrolled textural porosity, and often suffer from the problem of deactivation by pore plugging due to coke formation in microspores.[8] With the advent of mesoporous materials, the synthesis of mesoporous alumina with high surface area and narrow pore size distribution is promising for application enhancement of porous alumina.

Based on the surfactant templating synthetic strategy of mesoporous silicas, a wide range of synthesis procedures have now been documented for the preparation of mesoporous aluminas by utilizing cationic, anionic and non-ionic surfactant as the structural directing agents and/or templates. Lee *et al.* prepared mesoporous alumina using aluminum tri-*sec*-butoxide and CTAB (cetyl trimethyl ammonium bromide) in 1-butanol, and its pore size could be tuned by changing the amount of additive water and hydrothermal temperature.[9] Shih *et al.* reported that mesoporous alumina was synthesized by using aluminum sec-butoxide and tartaric acid in ethyl alcohol, and the mesoporous solid had narrow pore size which could be tailored by varying the concentration of the organic template of tartaric acid.[10] Yan *et al.* used Pluronic P123 and aluminium iso-propoxide in ethanol solvent to prepare mesoporous alumina, and its pore size could be adjusted by changing the type of acids and the chain length of block copolymers.[11] Even though many approaches for the preparation of mesoporous alumina with controllable pore size have been developed, but these methods usually employ the expensive and toxic aluminum alkoxides as the source of alumina in various organic solvents, which encounter the economical and environmental problems from the point view of practical application. For these reasons, it appears greatly attractive to synthesize mesoporous alumina by using inorganic aluminum salt as alumina source and water as solvent. However, the synthesis of thermally stable mesoporous alumina in aqueous media often represents a much more complex problem due to the susceptibility for hydrolysis as well as to the collapse of mesostructure upon removal of the template during calcination.[7,12] Therefore, it is still a challenge to obtain mesoporous alumina with high surface area, uniform and tunable pore size, and high thermal stability *via* a convenient and economic approach.

Plant tannins, a kind of natural polymer, are widely distributed in plant bark, leaf and fruit. Tannins have some surfactant-like characteristics and can be assembled into

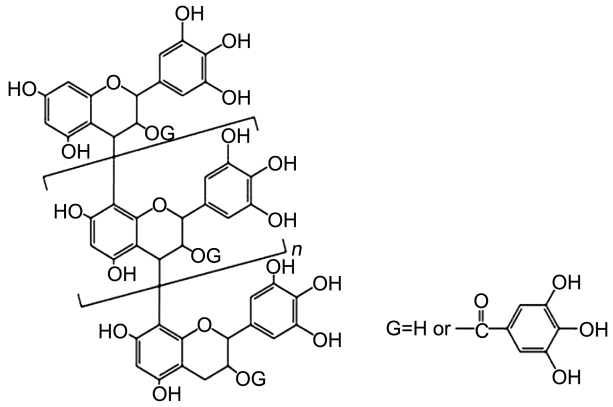

Figure 1. Molecular structure of bayberry tannin.

micelles in aqueous media.[13,14] The molecular structure of tannins consists of many adjacent phenolic hydroxyls, and it has been proved that tannins have the ability to chelate with many metal ions by the formation of five-membered chelated rings.[15,16] So, it can be expected that in aqueous solution containing inorganic aluminum salt and tannins, the micellated tannins would act as the structure-directing agent for the assembly of inorganic phase by chelating with Al species at hybrid interfaces. Moreover, the chelation reaction might provide the desired acting force to guide the formation of mesostructure during the self-assembly process of the organic and inorganic phase. To demonstrate this strategy, at the present investigation, bayberry tannin (Fig. 1) was used as the structure-directing agent and aluminium nitrate as source of alumina in aqueous media to synthesis mesoporous alumina. Furthermore, the as-prepared mesoporous alumina supported palladium catalyst was prepared by impregnation method, and its catalytic performance in the hydrogenation was also investigated.

Experimental

Reagents. $Al(NO_3)_3{\cdot}9H_2O$, palladium chloride ($PdCl_2$), propenol, styrene, linoleic acid, methanol and other chemicals were all analytic reagents and used without further purification. Bayberry tannin was obtained from the barks of *myrica esculenta* by extraction with an acetone/water solution (1:1, v/v) and then spray-dried. The tannin content of the extract was determined to be 76.3% according to the Hide Powder Method.[17]

Synthesis Procedure. A typical synthetic procedure is as follows: 47 mL of 0.8 mol/L $Al(NO_3)_3$ solution was mixed with 150 mL of BT solution (3 wt %) under vigorous stirring. The pH of the mixture was adjusted to 5.5 using ammonia aqueous solution (5 wt %). After 1 h stirring, the resulting suspension was transferred into a Teflon-lined stainless steel autoclave. The autoclave was heated to 150 °C (5 °C/min) and kept in isothermal condition for 48 h under N_2 atmosphere. After cooling down to room temperature naturally, the intermediate product, denoted as BT-Al, was collected after filtration, washed with distilled water and dried at 60 °C for 24 h. Finally, this intermediate product was ground to powder and calcinated at 600 °C for 6 h under air atmosphere to remove bayberry tannin, and the final product of mesoporous alumina (M-Al_2O_3) was obtained. The mesoporous aluminas with different pore sizes were prepared by adjusting the mass ratio of BT/$Al(NO_3)_3$, BT concentration, the pH value of reaction and hydrothermal temperature (see Tables 1-4). Thermal stability test of the as-prepared mesoporous alumina was performed by recalcinating it for 2 h at 800 and 900 °C, respectively. And the corresponding samples after recalcination were denoted as M-Al_2O_3-800 and M-Al_2O_3-900, respectively. For comparison, the reference alumina (R-Al_2O_3) was prepared using the similar method but without the use of bayberry tannin.

Catalyst Preparation. Supported palladium catalyst was prepared by impregnation method. 1 g of M-Al_2O_3 was mixed with 10.0 mL of 1.0 mg/mL Pd^{2+} solution under constant stirring at 25 °C for 24 h. The impregnated sample was collected after centrifugation, dried in ambient air at 60 °C for 24 h, then further reduced under 2.0 MPa H_2 at 200 °C for 2 h, and the final product, denoted as Pd-Al_2O_3*, was obtained. For comparison, the Pd-Al_2O_3 catalyst was prepared by using R-Al_2O_3 as support.

Characterization. The specific surface area and pore structure of samples were analyzed by N_2 adsorption/desorption using Surface Area and Porosity Analyzer of Micromeritics Tristar 3000. The powder X-ray diffraction patterns of samples were recorded by an X'Pert PRO MPD diffractometer (PW3040/60) with Cu-$K\alpha$ radiation. The morphology of samples was observed by Scanning Electron Microscopy on JSM-5900LV and Transmission Electron Microscopy on FEI-Tecnai G2.

Hydrogenation Reaction. All catalytic hydrogenation reactions were carried out in a Teflon-lined stainless steel autoclave (150 mL). Typically, the hydrogenation reactions of propenyl and styrene were performed at 30 °C and 1 MPa H_2 using methanol (20 mL) as solvent. The hydrogenation reaction of linoleic acid was performed at 80 °C and 2 MPa H_2 using the deoxygenated decane (50 mL) as solvent. The concentration of the reactants and products were analyzed by gas chromatograph (Shimadzu, CG-2010). The activity of the catalyst was evaluated according to the initial hydrogenation rate (mol/Pd mol h) value determined by the initial slope of the curve of product yield *vs.* time.[18]

Results and Discussion

Characterization of Mesoporous Alumina (M-Al_2O_3).

Textural Characterization. Figure 2 shows the nitrogen adsorption/desorption isotherms of representative sample (M-Al_2O_3), obtained when the mass ratio of BT/$Al(NO_3)_3$ was 0.32:1, pH was 5.5 and hydrothermal temperature was 150 °C. It can be observed that the adsorption/desorption isotherms of M-Al_2O_3 exhibit typical type IV curves, which is the characteristic of mesoporous material, and the H2-shaped hysteresis loop in the isotherms suggests the presence of "ink-bottle" type pores in M-Al_2O_3.[19] In addition,

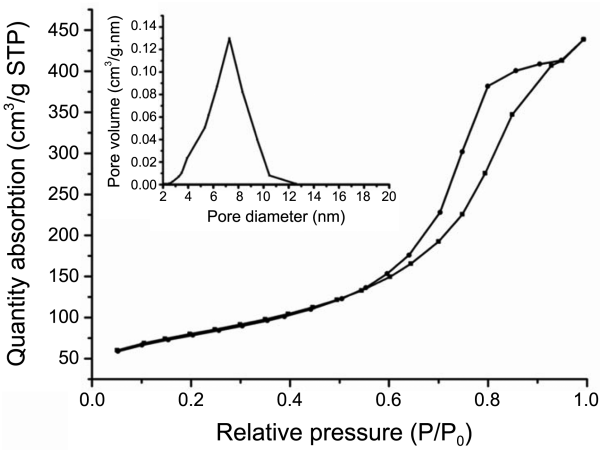

Figure 2. Nitrogen adsorption/desorption isotherms of M-Al_2O_3. Inset: pore size distribution of M-Al_2O_3.

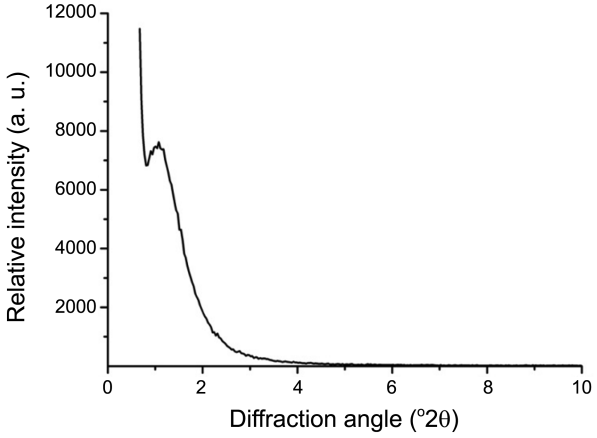

Figure 4. Low angel XRD patterns of M-Al_2O_3.

the physisorption measurement also reveals that M-Al_2O_3 had the relatively high BET surface area (281.3 m^2/g) and the narrow pore size distribution (shown in the inset of Fig. 2). In contrast, the low BET surface area (129.6 m^2/g) and the broad pore distribution were obtained for the reference sample of R-Al_2O_3 prepared without bayberry tannin (see Table 1 and Fig. 6). Therefore, the presence of bayberry tannin in the precursors of alumina is critical for the formation of the mesoporous structure with relatively high surface area and narrow pore size distribution.

XRD Patterns. In order to investigate the phase transformation during calcination, the crystal structure analysis of BT-Al and M-Al_2O_3 were performed by the wide angle XRD. As shown in Figure 3, the as-synthesized composite of BT-Al before calcination appears the diffraction patterns corresponding to boehmite (JCPDS Card 21-1307), while the calcined product of M-Al_2O_3 exhibits diffraction lines ascribing to γ-Al_2O_3 (JCPDS Card No. 10-0425), indicating the crystalline pore wall in M-Al_2O_3. For the application of alumina as catalyst support, this crystalline alumina synthesized by BT-templating method has definite superiority over the amorphous aluminas.[7,20] This is because those amorphous aluminas usually lack of the desired surface

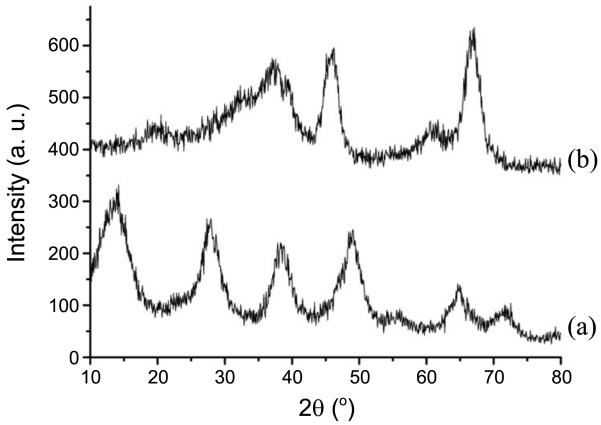

Figure 3. Wide angle XRD of BT-Al (a) and M-Al_2O_3 (b).

characteristic of a transition alumina phase and have limited hydrolytic stability. For instance, they quickly lose their mesostructure frameworks when suspended in water even at ambient temperature.[21]

The mesoporous character of M-Al_2O_3 was further verified by low angle XRD analysis. As shown in Figure 4, the diffraction pattern of M-Al_2O_3 emerges one low angle peak of 2θ around 1° corresponding to a *d*-spacing of 82 A, which is related to the presence of mesoporous structure with the uniform pore size rather than the long-range ordered pore arrangement. [22-24] Accordingly, based on the analysis of the low angle XRD and the nitrogen adsorption/desorption isotherms, it can be verified that the mesostructure of M-Al_2O_3 was effectively preserved during the removal of bayberry tannin by calcination. As we know that the molecular backbone of bayberry tannin mainly consists of rigid aromatic rings, and thus, one can reason that this desirable structure played a crucial role for preserving the mesostrucure of M-Al_2O_3 during calcination process, which can act as scaffold for the supporting of building blocks and provide the BT micelles with ability to resist the collapse of mesostructure.

SEM and TEM Characterization. The morphology of the alumina samples was observed by SEM and TEM. As shown in the Figure 5(a), the SEM image of M-Al_2O_3 prepared by BT-templating method appears relatively small nanoparticles. On the other hand, the SEM image of R-Al_2O_3 prepared without templating (Fig. 5(b)) exhibits the aggragates of larger nanorod. Figure 5(c) is the TEM image of M-Al_2O_3, it clearly shows that M-Al_2O_3 is built-up of very tiny corrugated nanoplatelets, and no discernible ordering of pores can be distinguished, however, its pores are reasonably uniform in size, which is in good with the absence of extra peaks in the low angle X-ray diffraction patterns. Further, the HRTEM image of M-Al_2O_3 in Figure 5(e) indicates the diameter of the nanoplatelets is less than 5 nm and the length varies from 5 to 22 nm. Figure 5(d) and Figure 5(f) are the TEM and HRTEM images of R-Al_2O_3, respectively. They reveal that R-Al_2O_3 appears in larger rod-shape particles which pile up randomly to form mesopores

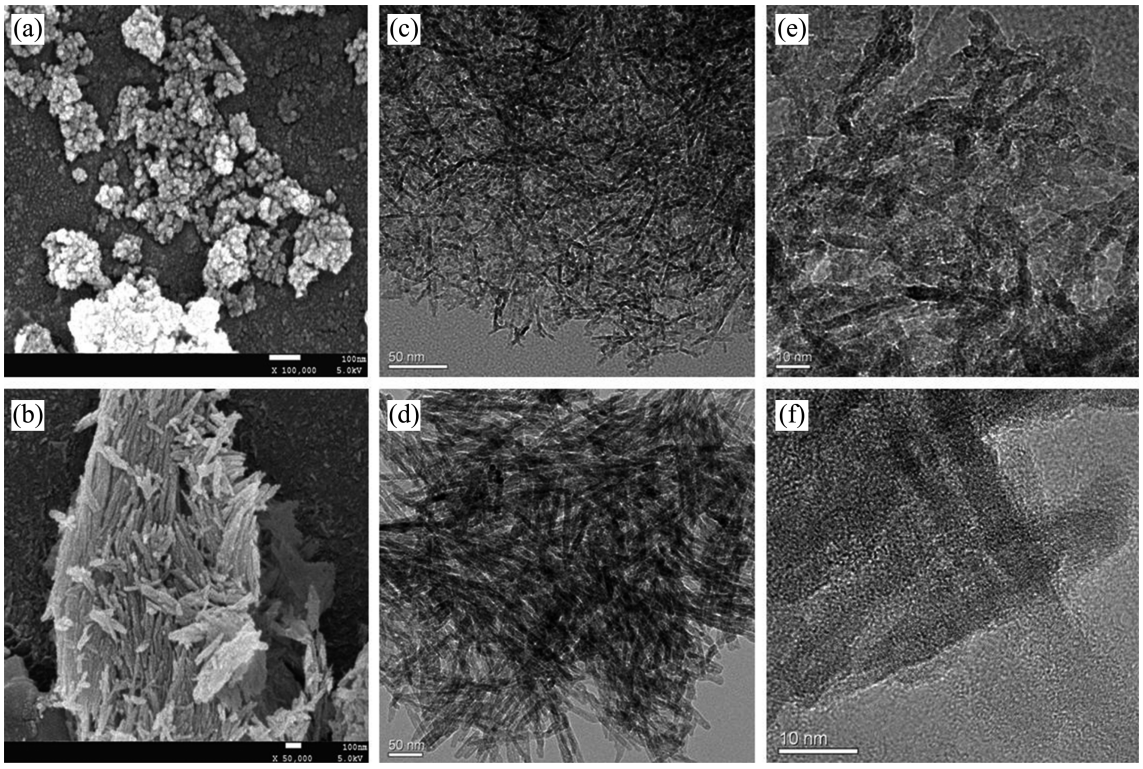

Figure 5. SEM images of M-Al_2O_3 (a) and R-Al_2O_3 (b); TEM images of M-Al_2O_3 (c) and R-Al_2O_3 (d); HRTEM images of M-Al_2O_3 (e) and R-Al_2O_3 (f).

with broad pore distribution.

It was documented that the hydrolysis rate of aluminum ions in aqueous media is ultra-fast, which leads to the formation of lamellar hydrated hydroxides even at the presence of surfactant.[25] However, the presence of bayberry tannin can greatly reduce this hydrolysis rate and inhibit the growth of lamellar hydrated hydroxide, as bayberry tannin has ability to chelate with alumina ion. In this way, the BT-Al^{3+} complex can be formed in the mixture of inorganic aluminum salt and bayberry tannin. Then, when $NH_3 \cdot H_2O$ was added, the hydrolysis of alumina ions was gradually preceded, and the slow hydrolysis process would be beneficial for the self-assembly process of aluminum hydroxide. That means the aluminum hydroxide clusters could be well-organized with the directing of BT micelles, which allows for the formation of mesoporous alumina with uniform pores. As a consequence, compared with R-Al_2O_3 prepared without templating, M-Al_2O_3 prepared with BT-templating appears to be built-up of tinier nanoplatelets with uniform pores.

The Effect of Experimental Parameters on the Structure of M-Al_2O_3. The mass ratio of BT/$Al(NO_3)_3$, BT concentration, the pH value of reaction and hydrothermal temperature would greatly influence the existing state of BT micelles, and the condensation and assembly process of aluminum species. Therefore, it is reasoned that the textual structure of mesoporous alumina can be adjusted by changing these experimental parameters.

Effect of the Mass Ratio of BT/$Al(NO_3)_3$. As indicated in Table 1, the specific surface area and pore volume of samples increase with increasing mass ratio of BT/$Al(NO_3)_3$, which implying the newly-built pores were generated by the removal of bayberry tannins. On the other hand, the pore volume of M-Al_2O_3-X (X=1-4) is not linearly increased with the increase of mass ratio of BT/$Al(NO_3)_3$, which proves that bayberry tannins were present in the form of micelles in aqueous solution.[14] Further, it is noticed that in Figure 6 the pore size distribution of M-Al_2O_3-1 and M-Al_2O_3-2 prepared

Table 1. Properties of mesoporous alumina synthesized with different BT/$Al(NO_3)_3$ mass ratio

Sample	BT/$Al(NO_3)_3$ mass ratio	BT concentration (%)	pH	T (^oC)	BET surface area (m^2/g)	Total pore volume (cm^3/g)	BJH pore diameter (nm)	Pore distribution (nm)
R-Al_2O_3	0	0	5.5	150	129.6	0.61	15.4	2.1-45.5
M-Al_2O_3-1	0.032:1	3%	5.5	150	154.4	0.57	24.1	4.8-31.6
M-Al_2O_3-2	0.064:1	3%	5.5	150	175.5	0.61	10.3	2.5-22.4
M-Al_2O_3-3	0.32:1	3%	5.5	150	281.3	0.78	7.8	2.8-12.4
M-Al_2O_3-4	0.48:1	3%	5.5	150	287.5	0.80	7.7	2.5-12.5

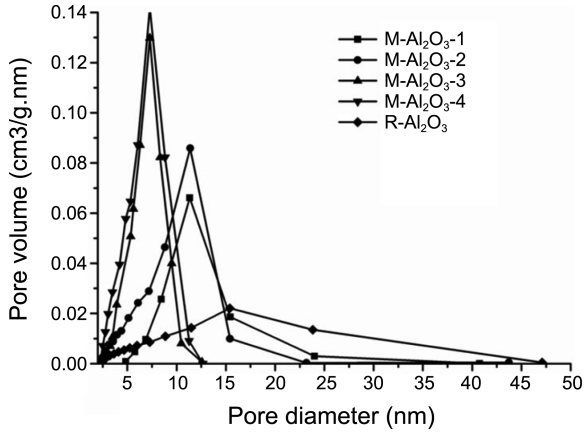

Figure 6. Pore size distribution of mesoporous alumina synthesized with different BT/Al$(NO_3)_3$ mass ratio.

with the BT/Al$(NO_3)_3$ mass ratio of 0.032:1 and 0.064:1, respectively, are very broad, while the narrow pore size distribution was observed in M-Al_2O_3-3 and M-Al_2O_3-4 prepared with the BT/Al$(NO_3)_3$ mass ratio of 0.32:1 and 0.48:1, respectively. These observations indicate that a sufficient amount of bayberry tannin was critical for the formation of the mesoporous alumina with relatively narrow pore distribution.

Effect of BT Concentration. As shown in Table 2, M-Al_2O_3-5 prepared with 1% BT concentration shows low specific surface area and pore volume, and broad pore size distribution, while M-Al_2O_3-6, M-Al_2O_3-7 and M-Al_2O_3-8 prepared with the BT concentration of 3% or above show relatively high specific surface area and pore volume, and narrow pore distribution. These phenomena are because that generally, for the obtained mesoporous material with good performance, the surfactant should be sufficiently higher than its critical micelle concentration (CMC). It was reported that the CMC of larch tannin is 0.184%.[26] Accordingly, the CMC of bayberry tannin should be around 0.184% considering its similar molecular structure with larch tannin. At low BT concentration of 1%, bayberry tannins in aqueous solution form aggregates with different sizes, and thus the hydrated aluminum hydroxide clusters directing by the BT aggregates are uneven and pile up randomly, which leads to the broad pore distribution of M-Al_2O_3-5. However, when the BT concentration is sufficiently higher than the CMC of bayberry tannin, the stable BT micelles with uniform size can be formed in the aqueous solution. As a consequence, the mesoporous aluminas with high surface area and narrow pore distribution were obtained, as shown for M-Al_2O_3-6, M-Al_2O_3-7 and M-Al_2O_3-8.

Effect of pH. pH has a great impact on the condensation rate of the inorganic phase[27] and the existing state of BT micelles, and thus significantly affect the textual structure of mesoporous alumina. In acidic condition, the BT micelles are stable, and the condensation rate of inorganic phase is lowered enough to allow the fabrication of the desired mesostructured aluminum oxide-hydroxide during the assembly process. Consequently, M-Al_2O_3-9 and M-Al_2O_3-10 prepared at pH of 4.5 and 5.5, respectively, have the high specific surface area and narrow pore distribution (Table 3). However, in the neutral condition, the condensation process of inorganic phase speeds up, and the fast formation process of inorganic network cannot match with the assembly process, which is unfavorable for the fabrication of desirable mesostructure. Moreover, the BT micelles are in negative charge at neutral pH, and these negatively charged BT micelles are easy to dissociate and form aggregates with different sizes due to the enhanced water-solubility and the electrostatic repulsion,[14] which further leads to the decrease of the specific surface area and the broad pore size distribution in M-Al_2O_3-11.

Effect of Synthesis Temperature. As can be seen from Table 4, the specific surface area and the pore size of mesoporous alumina increase with increasing synthesis temperature in the range of 25-150 °C. And it is worth pointing out that the specific surface area and the pore volume of mesoporous alumina are very low at 25 °C, suggesting the assembly process was not completed. However, when temperature is further raised to 200 °C, the specific surface area conversely decreases, and the pore size distribution becomes broad. These phenomena would be caused by the

Table 2. Properties of mesoporous alumina synthesized with different BT concentration

Sample	BT/Al$(NO_3)_3$ mass ratio	BT concentration (%)	pH	T (°C)	BET surface area (m^2/g)	Total pore volume (cm^3/g)	BJH pore diameter (nm)	Pore distribution (nm)
M-Al_2O_3-5	0.32:1	1%	5.5	150	215.1	0.67	9.3	2.0-31.5
M-Al_2O_3-6	0.32:1	3%	5.5	150	281.3	0.78	7.8	2.8-12.4
M-Al_2O_3-7	0.32:1	5%	5.5	150	279.8	0.72	6.8	2.0-13.2
M-Al_2O_3-8	0.32:1	7%	5.5	150	283.1	0.73	6.7	2.0-13.3

Table 3. Properties of mesoporous alumina synthesized at different pH value

Sample	BT/Al$(NO_3)_3$ mass ratio	BT concentration (%)	pH	T (°C)	BET surface area (m^2/g)	Total pore volume (cm^3/g)	BJH pore diameter (nm)	Pore distribution (nm)
M-Al_2O_3-9	0.32:1	3%	4.5	150	245.1	0.51	5.9	2.0-12.8
M-Al_2O_3-10	0.32:1	3%	5.5	150	281.3	0.78	7.8	2.8-12.4
M-Al_2O_3-11	0.32:1	3%	7	150	277.1	0.85	9.5	2.0-31.6

Table 4. Properties of mesoporous alumina synthesized at different temperature

Sample	BT/Al(NO$_3$)$_3$ mass ratio	BT concentration (%)	pH	T (°C)	BET surface area (m^2/g)	Total pore volume (cm^3/g)	BJH pore diameter (nm)	Pore distribution (nm)
M-Al_2O_3-12	0.32:1	3%	5.5	25	158.5	0.19	4.6	2.0-5.0
M-Al_2O_3-13	0.32:1	3%	5.5	100	193.3	0.46	7.6	2.3-10.2
M-Al_2O_3-14	0.32:1	3%	5.5	150	281.3	0.78	7.8	2.8-12.4
M-Al_2O_3-15	0.32:1	3%	5.5	200	233.8	0.73	9.1	2.8-28.8

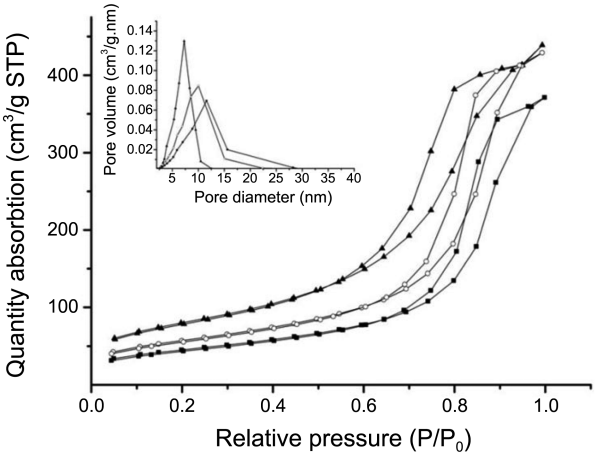

Figure 7. Nitrogen adsorption/desorption isotherms of M-Al_2O_3 (▲), M-Al_2O_3-800 (○) and M-Al_2O_3-900 (■). Inset: pore size distributions of the corresponding samples.

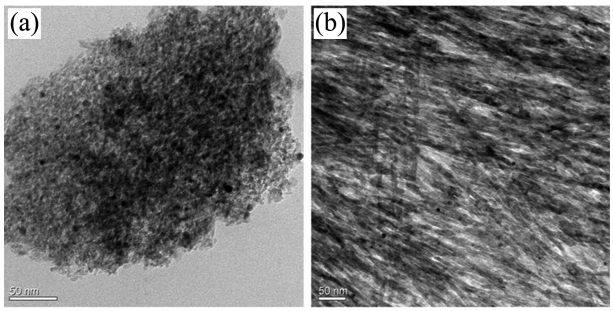

Figure 8. TEM micrographs of Pd-Al_2O_3* (a) and Pd-Al_2O_3 (b).

increasingly thermodynamical instability of the BT micelles at high temperature.

Investigation of Thermal Stability. The thermal stability of mesoporous γ-alumina has been studied by examining the stability of its physical properties after recalcination at higher temperature. Figure 7 shows the N_2 adsorption/desorption isotherms of M-Al_2O_3, M-Al_2O_3-800 and M-Al_2O_3-900. All the isotherms belong to type IV with small changes in the size of hysteresis loop and mesopore-filling position, indicating similar pore structures of M-Al_2O_3-800 and M-Al_2O_3-900 with M-Al_2O_3. On the other hand, the treatment of recalcination leads to decrease somewhat in the specific surface area and pore volume, but the relatively high specific surface area and pore volume are still maintained. As indicated in Table 5, the specific surface area and pore volume of M-Al_2O_3-900 are as high as 165.2 m^2/g and 0.58 cm^3/g, respectively. Furthermore, the recalcination at elevated temperature leads to the increase of pore size, the pore sizes of M-Al_2O_3-800 and M-Al_2O_3-900 are 9.4 and 10.7 nm, respectively. The increase of pore size is, however, accompanied by being broadening of the pore size distribution (shown in the inset of Fig. 7), which can be reasonably ascribed to the generation of larger pores in the re-sintering process. These results indicate that the mesoporous γ-alumina prepared by the BT-templating method is structurally stable for thermal treatment. The high thermal stability of the mesoporous γ-alumina enhances its potential application in catalysis.

Catalytic Hydrogenation. The mesoporous γ-alumina synthesized by the BT-templating method was examined as catalyst support in the hydrogenation of propenyl, styrene, and linoleic acid. Table 6 shows the catalytic reaction results of palladium supported on M-Al_2O_3-4 (Pd-Al_2O_3*) and for comparison, on the reference alumina (Pd-Al_2O_3). TEM images show that the average sizes of Pd particles are 7.2 nm and 7.5 nm on Pd-Al_2O_3* (Fig. 8(a)) and Pd-Al_2O_3 (Fig. 8(b)), respectively, indicating similar Pd dispersion on the two supports. As shown in Table 6, for all substrates, Pd-Al_2O_3* was found to be more active than Pd-Al_2O_3, which can be attributed to their difference in textual structure. Moreover, the catalytic activity advantage of Pd-Al_2O_3* over Pd-Al_2O_3 for the hydrogenation of those three reactants increased in the following order: propenyl < styrene < linoleic acid, which is in the same order of molecular size. These facts indicate that the advantage of Pd-Al_2O_3* is more obvious for the catalytic reaction of large molecular substrate. In case of the hydrogenation of linoleic acid, it was observed that 85.7% of the product was stearic acid at 90%

Table 5. Properties of M-Al_2O_3 heat treated at different temperatures

Temperature (°C)	BET surface area (m^2/g)	Total pore volume (cm^3/g)	BJH pore diameter (nm)	Pore distribution (nm)
600	281.3	0.78	7.8	2.8-12.4
800[a]	210.3	0.67	9.4	2.8-22.3
900[b]	165.2	0.58	10.7	2.8-28.2

[a]M-Al_2O_3 was treated by recalcinations at 800 °C for 2 h. [b]M-Al_2O_3 was treated by recalcinations at 900 °C for 2 h.

Table 6. Activities of supported palladium catalysts in hydrogenation of propenyl[a], styrene[a] and linoleic acid[b]

Substrate	Initial hydrogenation rate (mol mol h^{-1})		TOF advantage[e] (%)	Selectivity at 90% conversion (%)	
	Pd-Al_2O_3*	Pd-Al_2O_3		Pd-Al_2O_3*	Pd-Al_2O_3
propenyl	15156	10679	141.9	93.4[c]	91.7[c]
styrene	11316	7390	153.1	–	–
linoleic acid	1626	815	199.5	85.7[d]	54.3[d]

[a]Catalyst/substrate, 2.5 μmol/10 mmol; solvent, 20.0 mL methanol; temperature, 30 °C; H_2 pressure, 1.0 MPa; Stirring rate, 1200 rpm. [b]Catalyst/substrate, 8.46 μmol/1.78 mmol; solvent, 50.0 mL decane; temperature, 80 °C; H_2 pressure, 2.0 MPa; Stirring rate, 1200 rpm. [c]The selectivity to propanol. [d]The selectivity to stearic acid. [e]TOF advantage = (Initial hydrogenation rate of Pd-Al_2O_3*/Initial hydrogenation rate of Pd-Al_2O_3) – 100%

conversation on Pd-Al_2O_3*, while only 54.3% on Pd-Al_2O_3. It was reported that the Pd catalysts on supports with the pore diameter between 7 and 8 nm have high activity and selectivity for steric acid in the hydrogenation of linoleic acid[28] and sunflower oil.[29] The pore size effect of mesoporous aluminas, together with their controllable uniform pore structures, large surface areas and high thermal stability, provides their potential applications in shape-selective catalysis.

Conclusion

This work presented a facile precipitation method to fabricate mesoporous γ-alumina by using barberry tannin as template in aqueous system. The existence of bayberry tannin effectively retarded the ultra-fast hydrolysis of aluminum ions in aqueous solution. Moreover, barberry tannin acted as the structure-directing agent to guide the formation of mesostructure by their chelating interaction with aluminum hydroxide clusters. The mesoporous γ-alumina had high specific surface area, narrow pore size distribution and high thermal stability. Most importantly, the textural parameters of mesoporous alumina were easily to be modulated. In the hydrogenation reaction, the BT-templating mesoporous γ-alumina as catalyst support exhibited excellent performance, suggesting great potential applications in shape-selective catalysis.

Acknowledgments. We acknowledge the financial supports provided by the National Natural Science Foundation of China (21176161) and National High Technology R&D Program (2011AA06A108). And the publication cost of this paper was supported by the Korean Chemical Society.

References

1. Boissière, C.; Nicole, L.; Gervais, C.; Babonneau, F.; Antonietti, M.; Amenitsch, H.; Sanchez, C.; Grosso, D. *Chem. Mater.* **2006**, *18*, 5238.
2. Khalil, K. M. S. *Appl. Surf. Sci.* **2008**, *255*, 2874.
3. Li, J. R.; Kuppler, R. J.; Zhou, H. C. *Chem. Soc. Rev.* **2009**, *38*, 1477.
4. Huh, S.; Kim, S. J. *Bull. Korean Chem. Soc.* **2008**, *29*, 913.
5. Liu, X. F.; Oh, M.; Lah, M. S. *Inorg. Chem.* **2011**, *50*, 5044.
6. Motiei, L.; Kaminker, R.; Sassi, M.; van der Boom, M. E. *J. Am. Chem. Soc.* **2011**, *133*, 14264.
7. Xu, B. J.; Xiao, T. C.; Yan, Z. F.; Sun, X.; Sloan, J.; González-Cortés, S. L.; Alshahrani, F.; Green, M. L. H. *Micropor. Mesopor. Mater.* **2006**, *91*, 293.
8. Yu, M. J.; Li, X.; Ahn, W. S. *Micropor. Mesopor. Mater.* **2008**, *113*, 197.
9. Lee, H. C.; Kim, H. J.; Rhee, C. H.; Lee, K. H.; Lee, J. S.; Chung, S. H. *Micropor. Mesopor. Mater.* **2005**, *79*, 61.
10. Liu, X. H.; Wei, Y.; Jin, D. L.; Shih, W. H. *Mater. Lett.* **2000**, *42*, 143.
11. Bai, P.; Xing, W.; Zhang, Z. X.; Yan, Z. F. *Mater. Lett.* **2005**, *59*, 3128.
12. Cejka, J. *J. Appl. Catal., A* **2003**, *254*, 327.
13. Vázquez, G.; González-Álvarez, J.; López-Suevos, F.; Antorrena, G. *Bioresour. Technol.* **2003**, *87*, 349.
14. Shi, B.; Di, Y. *Plant Polyphenol*; Science Press: Beijing, China, 2000; p 138.
15. Yamguchi, H.; Higasida, R.; Higuchi, M.; Sakata, N. *J. Appl. Polym. Sci.* **1992**, *45*, 1463.
16. Sengil, I. A.; Ozacar, M. *J. Hazard. Mater.* **2009**, *166*, 1488.
17. Garro Galvez, J. M.; Riedl, B.; Conner, A. H. *Holzforschung* **1997**, *51*, 235.
18. Kacer, P.; Late, L.; Kuzma, M.; Cerveny, L. *J. Mol. Catal. A: Chem.* **2000**, *159*, 365.
19. Sangwichien, C.; Aranovich, G. L.; Donohue, M. D. *Colloids Surf., A* **2002**, *206*, 313.
20. Chaikittisilp, W.; Kim, H. J.; Jones, C. W. *Energy Fuels* **2011**, *25*, 5528.
21. Zhang, Z. R.; Pinnavaia, T. J. *J. Am. Chem. Soc.* **2002**, *124*, 12294.
22. Aguado, J.; Escola, J. M.; Castro, M. C. *Micropor. Mesopor. Mater.* **2010**, *128*, 48.
23. Morajkar, P. P.; Fernandes, J. B. *Catal. Commun.* **2010**, *11*, 414.
24. Kleitz, F.; Kim, T. W.; Ryoo, R. *Bull. Korean Chem. Soc.* **2005**, *26*, 1653.
25. Cabrera, S.; Haskouri, J. E.; Alamo, J.; Beltran, A.; Beltran, D.; Mendioroz, S.; Marcos, M. D.; Amoros, P. *Adv. Mater.* **1999**, *11*, 379.
26. Wang, Z.; Li, Z. Z.; He, X. N. *Bio. Chem. Eng.* **2006**, *40*, 31.
27. Soler-Illia, G. J. A. A.; Sanchez, C.; Lebeau, B.; Patarin, J. *J. Chem. Rev.* **2002**, *102*, 4093.
28. Maki-Arvela, P.; Kuusisto, J.; Sevilla, E. M.; Simakova, I.; Mikkola, J. P.; Myllyoja, J.; Salmi, T.; Murzin, D. Y. *Appl. Catal., A* **2008**, *345*, 201.
29. Belkacemi, K.; Boulmerka, A.; Hamoudi, S.; Arul, J. *Int. J. Chem. React. Eng.* **2005**, *3*, 59.